polysilazane. The efficient removal of C in the polymer by NH_3 produces a homogeneous distribution of stationary radical sites in the polymer. In contrast, graphite-rich regions containing mobile electrons are produced by the N_2 pyrolysis. Heating to temperatures as high as 1000 °C in NH_3, and to higher temperatures in N_2, causes both the loss of residual C and H and eventual crystallization of the amorphous Si_xN_y network to α-Si_3N_4.

Although the thermally induced dissociation of NH_3 is negligible below 650 °C, we observe significant N levels in the ceramic product isolated at 400 °C. This result implies that NH_3 is not thermally dissociated prior to reaction with the polysilane backbone. Our ESR results suggest that free radical sites produced at relatively low temperatures by decomposition of the polymer are scavenged by the NH_3 pyrolysis gas. NH_3 then serves as a radical transfer agent which can generate species that can subsequently react with the polymer to incorporate N.

Acknowledgment. The National Science Foundation is acknowledged for support under Materials Chemistry Initiative Grant No. CHE-8706131, along with the Colorado State University NMR Center, funded under NSF Grant No. CHE-8616437.

Nonlinear Optical Properties of Magnetically Aligned Solid Solutions of Nematic Polymers and Dye Molecules

S. I. Stupp,*[,†,‡,§] H. C. Lin,[†,‡] and D. R. Wake[‡]

Department of Materials Science and Engineering, Materials Research Laboratory, and Beckman Institute for Advanced Science and Technology, University of Illinois at Urbana—Champaign, Urbana, Illinois 61801

Received November 5, 1991. Revised Manuscript Received May 27, 1992

We have studied the second-order nonlinear optical response of a solidified nematic polymer containing a photoactive organic dye as a dissolved solute or as phase-separated crystals. Solvation of the dye in the main-chain nematic is evidenced by melting point depression with increasing dye concentration up to 20% by weight. Electrical poling of the dye–polymer alloy below the melting point of the nematic host results in strong second harmonic intensities from an infrared laser pulse passing through the medium. A comparison of thermally stimulated discharge spectra of poled alloys with nonlinear optical measurements indicates that dipolar ordering of solute molecules in the electric field gives rise to second harmonic activity. Interestingly, magnetically induced order in the nematic solvent can result in second harmonic signals which are 6–9 times more intense, equivalent to the second-order susceptibility of the system tripling. In this macroscopically organized environment, polar ordering of the dye solute in the electric field occurs more rapidly than in the polydomain nematic phase. Furthermore, the thermal stability of the polar dye network is greater as well in the aligned environment. The magnetically aligned nematic alloy can be regarded as an "Ising-like" medium in which the nematic and the magnetic fields confine dipolar dye molecules along directions parallel or antiparallel to the applied electric field. Previous calculations predict an increase of the second-order susceptibility by a factor of 5 in an idealized system as compared to a factor of 3 found in these experiments.

Introduction

In recent years there has been rising interest in the field of nonlinear optical properties of organic solids. This statement is supported by many contributions to the literature, including reviews on the subject.[1,2] One of the specific properties of interest has been second harmonic generation (SHG), that is, doubling of the frequency of laser beams as they pass through organic media. Provided various technical difficulties are solved, some are of the opinion that the nonlinear optical properties of organic materials may be useful in electrooptical technologies that transmit or store information through light beams. It is well-known that SHG-active organic materials contain molecules with strong electron donor and acceptor groups separated by conjugated bonds.[3] Many if not most of these photoactive molecules are therefore dyes that have a large dipole moment along their principal axis. The medium which doubles the frequency must also be noncentrosymmetric, implying the organic material must be a single crystal lacking an inversion center or a matrix in which an external electric field has been used to bias the spatial orientation of the molecular dipoles and thus to break the inversion symmetry.

This paper studies a noncentrosymmetric medium for SHG formed by polymers with nematogenic backbones as a solvent for photoactive dye solutes. We reported recently our initial results on the system.[4] The physical idea is to produce an "Ising-like" solution of nematic polymer and dye in an external magnetic field in order to generate a macroscopic director but with random up or down dipolar orientation. If dye molecules tend to align with the solvent's backbone and the magnetic field defines a macroscopic director, then the local symmetry of the polymeric

† Department of Materials Science and Engineering.
‡ Materials Research Laboratory.
§ Beckman Institute for Advanced Science and Technology.

(1) Ulrich, D. R. In *Organic Materials for Nonlinear Optics*; Hann, R. A., Bloor, D., Eds.; Royal Society of Chemistry: London, 1989; p 241.
(2) *Nonlinear Optical Properties of Organic Molecules and Crystals*; Chemla, D. S., Zyss, J., Eds.; Academic Press: New York, 1987; Vols. I and II.
(3) Nicoud, J. F.; Twieg, R. J. In *Nonlinear Optical Properties of Organic Molecules and Crystals*; Chemla, D. S., Zyss, J., Eds.; Academic Press: New York, 1987; p 227.
(4) Lin, H. C.; Wake, D.; Stupp, S. I. *Bull. Am. Phys. Soc.* **1990**, *35*, 560.

0897-4756/92/2804-0947$03.00/0

solvent reduces the spatial degrees of freedom of dye molecules. This forces dye molecules to sample prolate rather than spherical volumes, forming an "Ising solution" in which dye molecules have random up or down dipolar orientations. An external electric field can easily break inversion symmetry, aligning the dipoles along a preferred direction. In this work we have synthesized this medium and probed its SHG activity through the doubling of a 1064-nm beam to 532 nm.

Before proceeding to describe our experimental work, it is useful to describe briefly some of the fundamental principles of SHG. Nonlinear polarization of electrons in an isotropic medium can be induced by the strong electric fields of laser beams as described by the expansion

$$P = \chi^{(1)}E + \chi^{(2)}E^2 + \chi^{(3)}E^3 + \ldots \quad (1)$$

where $\chi^{(1)}$ is the linear susceptibility and the others nonlinear ones. The part of the polarization associated with nonlinear terms gives rise to the generation of optical harmonics.[5,6] In anisotropic media, where P and E are not necessarily parallel

$$P_I = \chi^{(1)}_{IJ}E_J + \chi^{(2)}_{IJK}E_JE_K + \chi^{(3)}_{IJKL}E_JE_KE_L + \ldots \quad (2)$$

where χ's are now susceptibility tensors and the components of the $\chi^{(2)}$ tensor are all zero in media with an inversion center. When this inversion center is absent, the nonlinear polarization response can result in energy exchange between fields of different frequencies. SHG specifically occurs when part of the energy of a wave of frequency ω propagating through the medium is converted to the energy of a 2ω wave. The equivalent "molecular" expression for nonlinear optical response is given by

$$P_i = \alpha_{ij}E_j + \beta_{ijk}E_jE_k + \gamma_{ijkl}E_jE_kE_l + \ldots \quad (3)$$

where α is the linear polarizability of the molecule and β and γ are known as the second and third nonlinear optical hyperpolarizabilities. Here β must again be zero when molecules possess a center of inversion.

The photoactive dye used in our work was the azo dye 4-[ethyl(2-hydroxyethyl)amino]-4′-nitroazobenzene (disperse red 1):

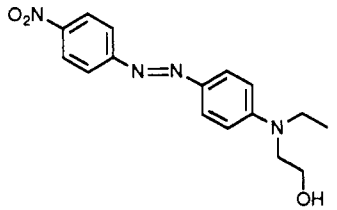

The macromolecular host of the dye was a chemically aperiodic nematic polymer containing the following three structural units:

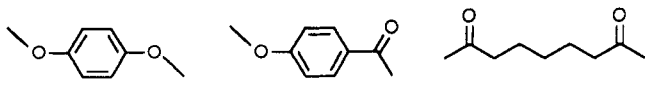

The ester bonds linking the units lead to semiflexible chains which form a nematic phase in the temperature range 185–220 °C (this range may extend below 185 °C), and above 220 °C a nematic–isotropic biphasic fluid is observed. Our group has published previously on the synthesis and characterization of this nematic polymer.[7] Characterization of the polymer–dye alloys was carried out by differential scanning calorimetry (DSC), thermally stimulated discharge (TSD), and second harmonic generation measurements.

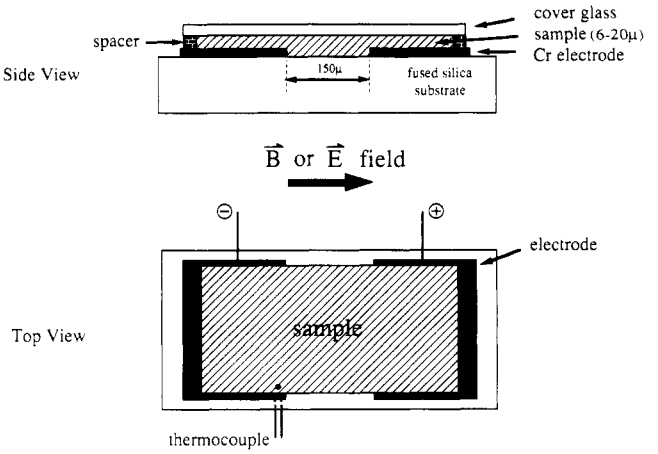

Figure 1. Schematic representation of the substrate used for samples in second harmonic generation measurements.

Experimental Section

Sample Preparation and Characterization. The photoactive dye 4-[ethyl(2-hydroxyethyl)amino]-4′-nitroazobenzene was obtained from Aldrich, and before use it was refluxed in acetone and recrystallized. Samples containing the liquid-crystal polymer and dye were prepared with different weight percents covering the range 1–80% dye. The liquid-crystal polymer was synthesized by J. Wu of our laboratory, and its synthesis and characterization are described elsewhere.[7] Preparation of all samples involved mixing both components above their melting temperatures, near 180 °C.

Samples for nonlinear optics (NLO) were prepared by first depositing thermally a thin conductive layer of chromium (2000–4000 Å) on a 1-mm-thick fused-silica slide. A 150-μm gap was etched by photolithography to form Cr thin-film electrodes on either side of the gap. This configuration of the NLO sample has been previously described by Boyd et al.[8] The polymer–dye alloy was placed (~1 mg) in the gap of a preheated fused-silica–Cr substrate (maintained above the melting point of the polymer–dye alloy). A Teflon spacer was then placed on the sample to control thickness and covered with a glass slide. A solid film 6–20 μm thick formed after cooling to room temperature at an approximate rate of 100 °C/min, and the sample was sealed around the edges with epoxy. A schematic of the sample cell is shown in Figure 1. Samples were analyzed in a Leitz Laborlux 12 POL polarizing microscope, and their thermal behavior was characterized using a Perkin-Elmer DSC-4 differential scanning calorimeter (samples weighed 4–6 mg and were heated at 10 °C/min).

Magnetic Alignment. Some samples placed on the fused-silica–Cr NLO substrates were aligned magnetically in the melt state using a Varian XL-200 NMR instrument equipped with a variable-temperature unit. The sample cell was placed in a specially designed holder to retain alignment of the electrode gap relative to the instrument's magnetic filed. In all cases the magnetic field direction was from one chromium electrode to the other. The samples were melted by heating to 180 °C and kept at this temperature for 15 min under the influence of the magnetic field. The magnetic field had an intensity of 4.7 T and was maintained during cooling of the samples to room temperature. Whenever comparisons were made between aligned and unaligned samples, the unaligned samples were subjected to the same thermal history followed for magnetic orientation, but in zero field. The control samples were prepared in a thermal bath purged with nitrogen and coupled to a temperature controller.

Nonlinear Optics. The experimental setup for poling samples and obtaining SHG measurements is shown in Figure 2. Samples

(5) Yariv, A. *Optical Electronics*, 3rd ed.; Wiley: New York, 1985.
(6) Fowles, G. R. *Introduction to Modern Optics*, 2nd ed.; Holt, Rinehart and Winston: New York, 1975.
(7) Moore, J. S.; Stupp, S. I. *Macromolecules* **1987**, *20*, 273.
(8) Ender, D. A.; Moshrefzadeh, R. S.; Boyd, G. T.; Leichter, L. M.; Liu, J. T.; Henry, R. M.; Williams, R. C. In *Nonlinear Optical Properties of Organic Materials*; Khanarian, G., Ed.; *SPIE* **1988**, *971*, 144.

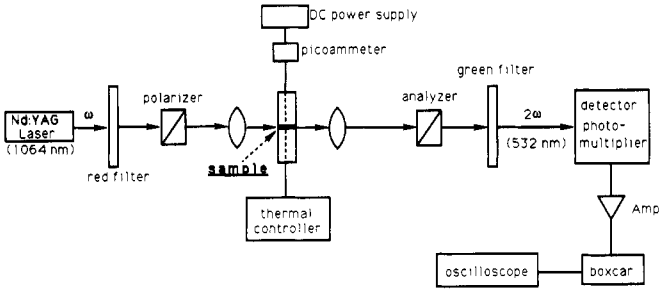

Figure 2. Experimental setup for second harmonic generation measurements.

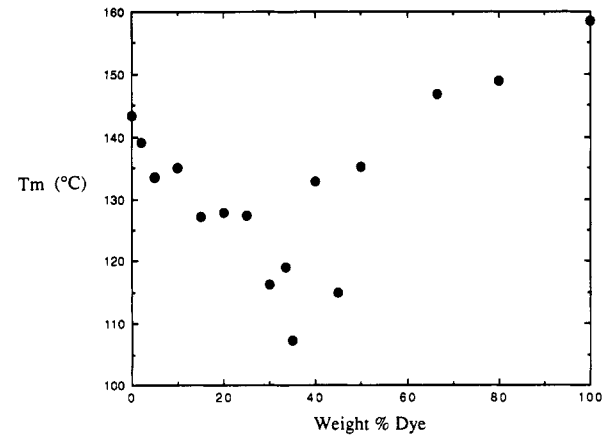

Figure 3. Melting temperatures of samples containing the nematic polymer and various weight percents of the photoactive dye.

were poled between the two chromium electrodes under a field of 67 kV/cm at 100 °C for 15 min. Light pulses of duration 15 ns at a repetition rate of 20 Hz from a Molectron Q-switched YAG:Nd laser (Model MY 34-20) with incident wavelength 1064 nm (ω) passed through the sample to generate an SHG signal with output wavelength 532 nm (2ω). The typical incident power used was 8.4 MW/cm^2 per pulse, with the beam focused using a cylindrical lens to a slit approximately 3 mm by 50 μm. The input beam polarization was adjusted by a Fresnel rhomb, and the polarization of the SHG beam was checked by an analyzer and spectrally filtered from the fundamental plus second harmonic beam using high-pass and notch filters. The signal was detected by a photomultiplier and measured on an oscilloscope. During the SHG experiment the incident power was continuously monitored and the SHG signal was verified by appropriate filters to ensure that it was generated by the sample. A quartz crystal with a value of $\chi^{(2)} = 1.9 \times 10^{-9}$ esu[9] was used as a reference to obtain $\chi^{(2)}$ values of the samples. Second harmonic generation signals were measured after the electric field was turned off at room temperature and during subsequent heating at an approximate rate of 10 °C/min. In some experiments SHG measurements were obtained from previously unpoled samples while heating under the influence of the electric field.

Thermally Stimulated Discharge. Thermally stimulated discharge experiments were carried out on samples melted between two pieces of conducting In_2O_3 glass serving as electrodes. The In_2O_3 glass was sputtered with gold on the edges and top surfaces in order to obtain conductive contact with the TSD electrodes. Mica spacers were used to control the thickness of the film (~10 μm). A Toyo Seiki TSD apparatus was used for polarization and thermal discharge of the polymer–dye alloys. In this instrument, polarization is induced within an insulated chamber filled with nitrogen gas using one stationary and one spring-loaded gold electrode. The field used in TSD experiments was 100 kV/cm and was applied at 100 °C for 15 min. The samples were then cooled under the field to −20 °C using liquid nitrogen. The thermal discharge current was measured with a picoammeter at a heating rate of 2 °C/min.

(9) *Handbook of Lasers*; Pressley, R. J., Ed.; Chemical Rubber Co.: Cleveland, 1971.

Table I. Maximum Temperatures (°C) of Endotherms in Nematic Polymer–Dye Alloys with Varying Weight Percents of Dye

endotherm	20%	25%	30%	40%	50%
I	113	119	95	100	107
II	128	128	117	133	136

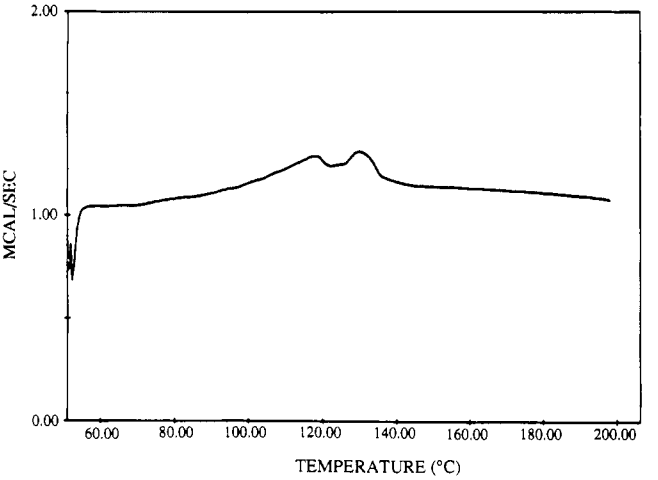

Figure 4. DSC of a sample containing 80% by weight of the nematic polymer and 20% dye.

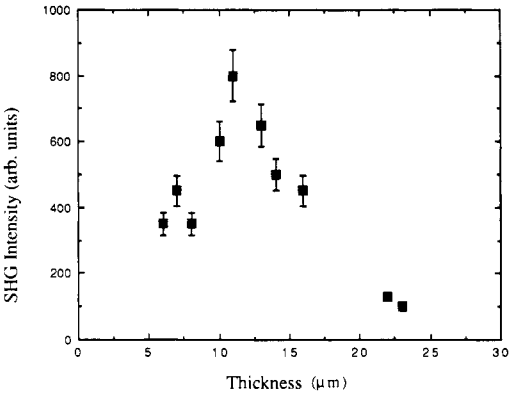

Figure 5. Second harmonic intensities generated by samples containing 2% by weight dye as a function of sample thickness.

Results and Discussion

Figure 3 shows a plot of melting points measured by DSC for nematic polymer–organic dye alloys of different compositions as well as those of the pure polymer and pure dye. The temperatures plotted correspond to the maximum temperature of the main endotherm in the DSC scan (T_{max}). The gradual decrease of the melting point with increasing dye content indicates the main-chain nematic polymer is a good solvent for the dye. At dye concentrations between 15% and 50% by weight, phase separation appears to occur in the system as indicated by the presence of two endotherms in the DSC scan. A typical scan in this range and T_{max} values for both endotherms are shown in Figure 4 and Table I, respectively. At very high dye concentrations, one observes melting points near that of the pure dye crystals. This study examined the nonlinear optical properties only of alloys containing low concentrations of dye, in the range 1–5 wt %. On the basis of the DSC data, we expect the formation of polymer–dye solid solutions within this concentration range.

Once poled in the external electric field, the nematic polymer–dye alloy films displayed significant second

Table II. Second-Order Susceptibilities [$\chi^{(2)}_{zzz}$ (esu)] of Nematic Polymer–Dye Solid Alloys Derived from Magnetically Aligned and Unaligned Liquids

	dye content, wt			
	0%	1%	2%	5%
$\vec{B}$-field unaligned	0.9×10^{-10}	5.96×10^{-10}	6.52×10^{-10}	1.51×10^{-9}
$\vec{B}$-field aligned	1.2×10^{-10}	1.19×10^{-9}	1.31×10^{-9}	4.53×10^{-9}

harmonic activity. Figure 5 shows that the relative SHG intensity rises with increasing film thickness to a thickness of approximately 12 μm. Increasing the film thickness beyond 12 μm causes a decrease in SHG intensity. Generally, an SHG-active material of thickness less than its coherence length generates a 2ω intensity which increases as the square of the material's thickness. A path length in the active medium that is longer than the coherence length causes the generated 2ω intensity to decrease and then oscillate with increasing thickness. The data shown in Figure 5 imply that the data spanning the thickness range 5–10 μm for our samples are within the first coherence length.

$\chi^{(2)}$ values for the various samples were calculated as follows using quartz as a reference and neglecting absorption:

$$\chi^{(2)} = 1.9 \times 10^{-9}(20\ \mu\text{m}/d)(I^{2\omega}/I_q^{2\omega})^{0.5} \qquad (4)$$

where $\chi^{(2)}$ is the second-order susceptibility of the sample in esu, d is the thickness of the sample in μm, and $I^{2\omega}$ and $I_q^{2\omega}$ are the second harmonic intensities of the sample and quartz reference, respectively. The value of 1.9×10^{-9} esu is the $\chi^{(2)}$ value of quartz and 20 μm corresponds to the coherence length of quartz. Table II shows the values of $\chi^{(2)}$ measured for three different alloys and also that of the pure nematic polymer.

Interestingly, we found a significant increase in the SHG signal in alloys which had been aligned by an external magnetic field prior to poling by the electric field. Figure 6 shows two optical micrographs of NLO samples containing 2% dye, revealing clearly a change in microscopic texture as a result of magnetic alignment. The overall transmission in the visible is not significantly increased however. We tested whether the enhanced $I^{2\omega}$ of films after magnetic orientation could be simply due to a decrease in absorption or scattering in the sample in the IR by measuring the attenuation of a beam of 1064 nm (ω) on passing through the sample. We did not find a significant difference in the value of I^{ω} passing through films that were magnetically aligned relative to films that were not aligned. Nonetheless, the intensity of the second harmonic generated from the fundamental beam in magnetically aligned alloys increased by a factor ranging from 6 to 9 as shown by data in Figure 7. Given this increase, $\chi^{(2)}$ is effectively tripled in 5% dye samples when the high molar mass solvent is macroscopically ordered in the magnetic field. $\chi^{(2)}$ data for both magnetically aligned and unaligned samples are shown in Table II.

Earlier work in our laboratory[10] showed that the nematic polymer used here can be aligned in magnetic fields and macroscopic order parameters $\langle S_{zz}^2 \rangle$ on the order of 0.5–0.7 can be obtained. We thus interpret the enhanced nonlinear optical activity in magnetically aligned samples as the result of some coupling between the macroscopic order parameter of the semirigid solvent chains and the field-induced polar ordering of dye molecules producing $C_{\infty v}$ symmetry in the system. Because of the anisotropic diamagnetic susceptibility of the nematic polymer, magnetic alignment leads to uniaxial orientation of the solvent chains, and this way may also promote some axial preference in the solute. In the extreme of a macroscopic order parameter approaching 1.0, the magnetic field would produce an "Ising" solution of nematic polymer and dye in which external poling would simply bias each chromophore's dipole moment parallel rather than antiparallel to

(10) Moore, J. S.; Stupp, S. I. *Macromolecules* **1987**, *20*, 282.

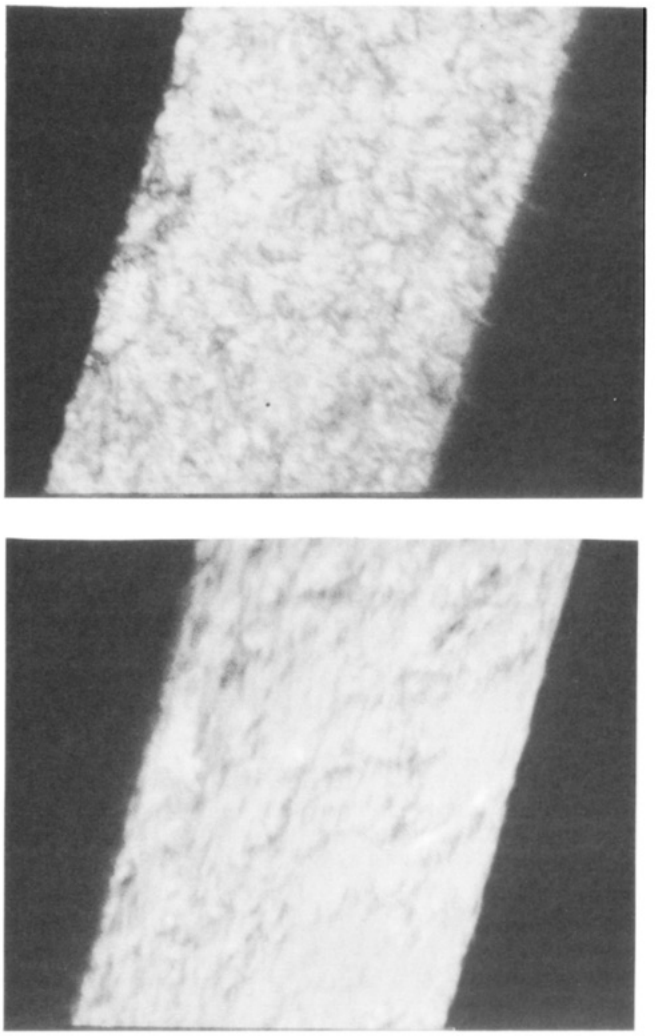

Figure 6. Optical micrographs of two NLO samples revealing the development of an oriented texture in the sample after magnetic alignment (bottom). The top micrograph corresponds to that of an unaligned sample.

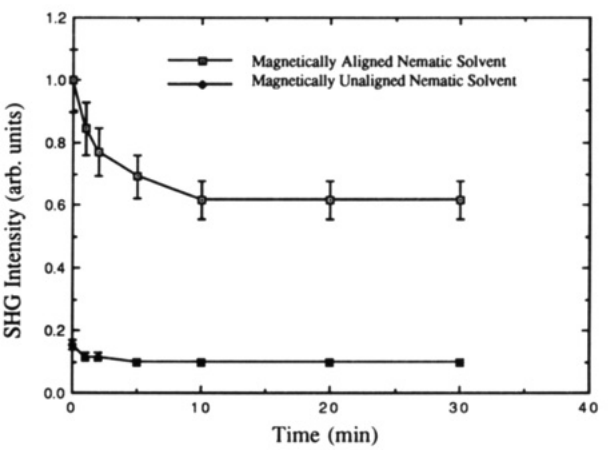

Figure 7. Effect of magnetic orientation on second harmonic intensity generated by samples containing 5% by weight dye. The second harmonic intensity is plotted in this curve as a function of time elapsed after removal of the poling electric field.

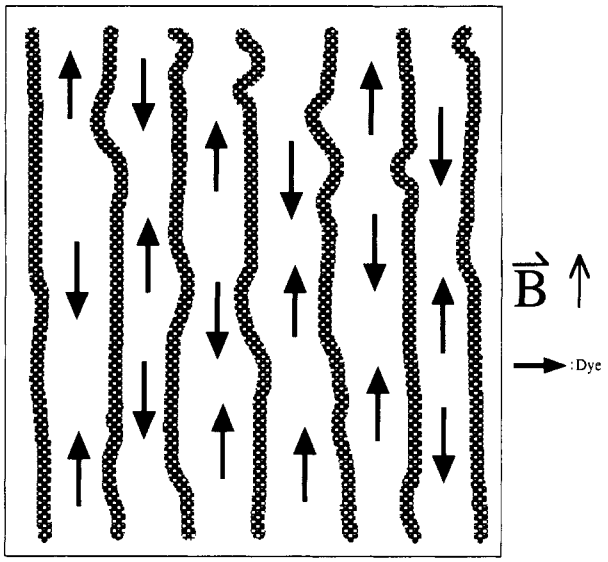

Figure 8. Schematic representation of the Ising solution of nematic polymer and dye formed in a magnetic field.

the electric field (see illustration in Figure 8). This concept is described below through a number of expressions quantifying the effect of order parameter on $\chi^{(2)}$.

The macroscopic susceptibility $\chi^{(2)}$ is related to molecular hyperpolarizability β by the following expression:

$$\chi^{(2)} = N\beta f(\omega_i)\, f(\omega_i)\, f(2\omega_i)\, O(\theta,\phi) \quad (5)$$

where N is the number density of photoactive molecules, $f(\omega_i)$ is the local field at frequency ω_i, and $O(\theta,\phi)$ is an orientation factor that projects β onto the macroscopic framework (θ is the angle between the dye z axis and the poling direction, and ϕ is a spherical polar coordinate). $\chi^{(2)}_{zzz}$ and $\chi^{(2)}_{zxx}$ are the only components of $\chi^{(2)}$ that do not vanish in poled polymer films, and thus assuming $\beta = \beta_{zzz}$ (the predominant component of the molecular tensor) and also that the z axis of the molecule is parallel to the molecular dipole moment that interacts with the orienting field (z direction)

$$\chi^{(2)}_{zzz} = N\beta F\langle(\mathbf{k}\cdot\mathbf{K})(\mathbf{k}\cdot\mathbf{K})(\mathbf{k}\cdot\mathbf{K})\rangle = N\beta F\langle\cos^3\theta\rangle \quad (6)$$

where $\mathbf{k}$ is the unit vector along the molecular z direction, $\mathbf{K}$ is the vector parallel to the poling (z) direction, and F is the product of all local field factors, i.e., $f(\omega_i)\, f(\omega_i)\, f(2\omega_i)$.

Under high-field situations and high concentration, Kielich[11] derived a generalized Langevin function that takes all factors into account:

$$O(\theta,\phi) = L_n(a,\pm b) = \int_0^\pi (\cos^n\theta)\exp(a\cos\theta \pm b\cos^2\theta)\sin\theta\, d\theta \Big/ \int_0^\pi \exp(a\cos\theta \pm b\cos^2\theta)\sin\theta\, d\theta \quad (7)$$

where $a = \mu E_d/kT$, E_d is the electric field with local field corrections, and b for an axial system is $E_d^2\epsilon_a/2kT$, where ϵ_a is the dielectric anisotropy, $\epsilon_a = \epsilon_\parallel - \epsilon_\perp$, and $\epsilon_\parallel$ and $\epsilon_\perp$ are the dielectric constants parallel and perpendicular to a nematic director. When $n = 3$ and $b = 0$, $L_3(a,\pm b)$ is given by

$$L_3(a,0) = a/5 - a^3/105 \quad (8)$$

$$\chi^{(2)}_{zzz} = N\beta F L_3(a) \quad (9)$$

Equation 8 applies to unsaturated alignment or the low-field limit ($\mu E/kT \ll 1$) and also systems of low anisotropy. $L_3(a)$ in eq 9 is the third-order Langevin function and $a = f(o)\mu E/kT$ where $f(o)$ is a local field factor. The values of $\langle\cos^3\theta\rangle$ and $\chi^{(2)}_{zzz}$ in a medium which is isotropic are given by

$$\langle\cos^3\theta\rangle_{isotropic} = \mu E/5kT \quad (10)$$

$$(\chi^{(2)}_{zzz})_{isotropic} = \frac{N\beta F\mu E}{5kT} \quad (11)$$

We must now predict the equivalent expression for $\chi^{(2)}_{zzz}$ in an externally aligned host and should therefore apply to what we call here the ideal Ising solution. This expression was derived by Meredith et al.,[12] showing that

$$\langle\cos^3\theta\rangle_{Ising} = \mu E/kT \quad (12)$$

$$(\chi^{(2)}_{zzz})_{Ising} = N\beta F\mu E/kT \quad (13)$$

Additional details of the derivation of expression 12 are described in the Appendix.

The expressions developed above indicate, as first shown by Meredith et al.,[12] that all other factors being equal, $\chi^{(2)}_{zzz}$ of a perfectly oriented polymer–dye solution should be 5 times larger than that of the isotropic system. Therefore our experimental observation of a tripled $\chi^{(2)}$ value in magnetically aligned polymer–dye alloys lies within the predicted factor of 5 for an ideal system. Most likely the observed factor of 3 is linked to the limited macroscopic order parameter ($\langle S^2_{zz}\rangle \sim 0.6$–$0.7$) attained magnetically in the polymer solvent used.[10]

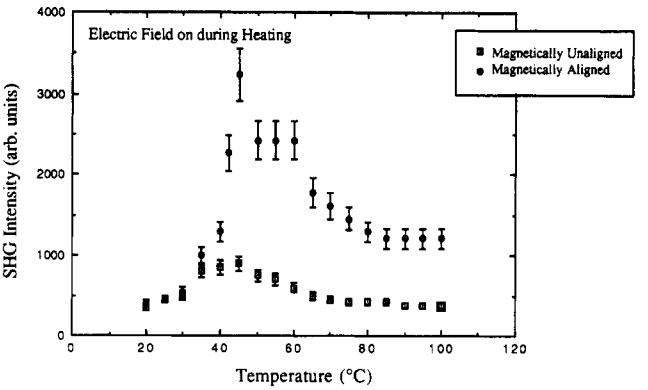

Figure 9. Second harmonic intensity as a function of temperature during poling of a sample containing 2% by weight dye. In one sample the nematic solvent was macroscopically aligned in a magnetic field. The second sample was unaligned and represents the corresponding thermal control of the aligned sample.

Figure 9 (lower curve) shows the increase in second harmonic intensity as a function of temperature in one of the magnetically unaligned samples under the influence of the external electric field. The experiment reveals the dynamics of symmetry breaking in the medium since this particular sample had not been previously poled. The SHG activity is immediately detected upon application of the field at room temperature and increases with temperature reaching a maximum near 45 °C. It is known from our previous work that near 40 °C the pure nematic polymer used here shows evidence of molecular motion by torsion braid analysis.[13] This indicates that chromophores are detrapped in the frozen solvent to break symmetry at

(11) Kielich, S. *IEEE J. Quantum Electron* **1969**, *QE-5*, 562.

(12) Meredith, G. R.; Van Dusen; Williams, D. J. *ACS Symp. Ser.* **1983**, *233*, 109.

(13) Stupp, S. I.; Moore, J. S.; Chen, F. Molecular Organization in Nematic Polymers. 2. Evolution of the Mesophase. *Macromolecules* **1991**, *24*, 6408.

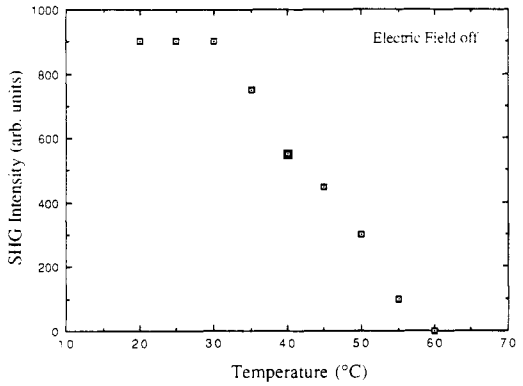

Figure 10. Second harmonic intensity as a function of temperature in the absence of an electric field in a sample containing 1% by weight dye.

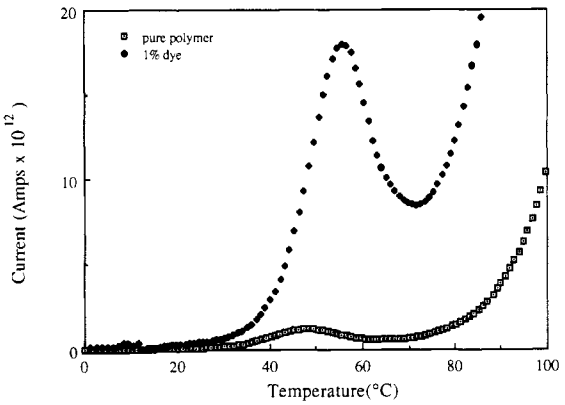

Figure 11. Thermally stimulated discharge spectra of poled samples, one containing only the nematic polymer and the other containing 1% by weight dye.

the onset of such motions. When poled samples are heated in the absence of the electric field (Figure 10), one observes that centrosymmetry is recovered in a similar thermal range. However, the relaxation of polar ordering in the absence of the field is observed to begin at temperatures when a significant amount of order had already occurred in the presence of the field. This could be explained in part by the electric interaction energy in the presence of the field and perhaps by some degree of thermal stability due to polar order in the dye network of poled samples. Interestingly in Figure 11 we show that the relaxation of polar order with temperature is also revealed by TSD of a poled sample. This figure shows a well-defined depolarization peak in a previously poled sample coinciding in temperature with the rapid loss of SHG signal. We interpret the data as demonstrating that dipolar chromophores with bias orientation along the external field randomize as molecular motions are thermally activated. Figure 11 also shows the TSD spectrum of the pure nematic polymer. A comparison of both curves shows clearly that the strong depolarization current is linked directly to the polar orientation of dye molecules in the electric field.

An important difference was observed in poling dynamics between magnetically aligned and unaligned samples. Figure 9 shows a plot of $I^{2\omega}$ as a function of increasing temperature in aligned and unaligned samples exposed to an electric field. The figure suggests that a greater rate of polar ordering of dye molecules occurs in the environment of an organized solvent. This difference supports the premise that dye molecules are themselves preordered in the uniaxial environment of the solvent, thus facilitating the removal of an inversion center by the electric field. As

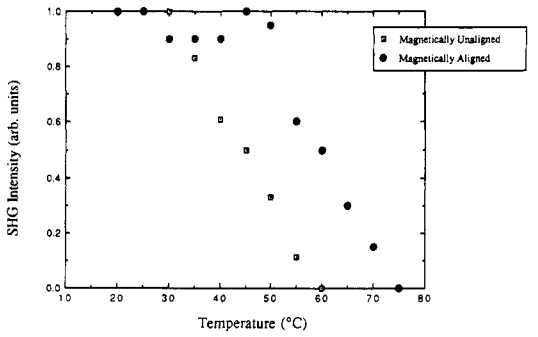

Figure 12. Fractional loss of the second harmonic intensity as a function of temperature in poled samples containing 1% by weight dye. One sample was aligned in a magnetic field before poling.

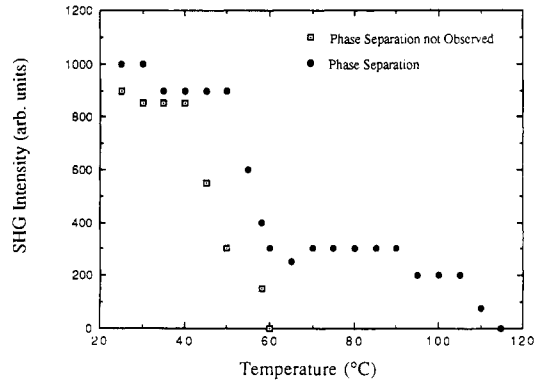

Figure 13. Second harmonic intensity as a function of temperature in samples containing 2% by weight dye. Dye phase separation was observed by optical microscopy in one sample.

expected from data presented in Figure 9, the final value of $I^{2\omega}$ reached as the temperature approaches 100 °C is greater in magnetically aligned samples. Furthermore, data in Figure 12 suggests that the thermal stability of the polar dye network is greater in aligned samples as well. This is revealed by the slightly higher thermal stability of the noncentrosymmetric medium in magnetically aligned samples.

Interestingly we found that some samples retained a measurable SHG signal at higher temperatures (above 60 °C). All cases in which this additional thermal stability of the SHG signal was found showed microscopic evidence of dye phase separation. Figure 13 shows the persistence of the SHG activity in a phase-separated sample above 60 °C compared to the thermally activated loss of SHG activity in a homogeneous sample. As melting of the dye–polymer alloy is approached, we observe in these samples the complete disappearance of the SHG signal. We were not able to define the exact thermal schedules that would reliably produce phase separation. However, phase separation appears to occur as alloys are heated beyond the melting point of the nematic polymer and then cooled to room temperature in the electric field. Exactly what determines the appearance of the phase-separated structure is not known at the moment. This is most likely related to local heating or cooling rates, sample thickness, and possibly the nature of the surfaces in contact with the alloy sample. Figure 13 shows a comparison of the thermally activated loss of $I^{2\omega}$ in a homogeneous sample and in a phase separated sample.

Conclusions

Dye molecules dissolved in a nematic polymer frozen in a magnetic field form solid films with $\chi^{(2)}$ susceptibility values that are 2–3 times larger than those solidified in the

absence of the field. This susceptibility enhancement points to coupling between polar ordering of dye molecules in the electric field and the uniaxial organization of the nematic solvent in a magnetic field. Additional evidence of this coupling is revealed in magnetically aligned samples by a more rapid rise of the second harmonic intensity with increasing temperature under the electric field. In an ideal system the magnetically aligned nematic alloy can be regarded as an "Ising-like" medium in which the nematic and external fields confine dipolar dye molecules along directions parallel or antiparallel to the electric field.

Acknowledgment. This project was funded by the U.S. Department of Energy through Grant No. DEFG02-91ER45439 to the University of Illinois Materials Research Laboratory. Partial funding in the early stages was also provided by 3M Co. We acknowledge J. Wu of our laboratory for the synthesis of the nematic polymer and Gary Boyd of 3M for helpful advice on the NLO experimental setup.

Appendix

The order parameter of the nematic solvent and the dissolved chromophore would be given by

$$S = \langle (3\cos^2\theta - 1)/2 \rangle = \int_0^\pi p(\theta)[(3\cos^2\theta - 1)/2] \sin\theta \, d\theta / \int_0^\pi p(\theta) \sin\theta \, d\theta \quad (14)$$

where θ is the angle of molecules with respect to the director axis, and $p(\theta)$ is the distribution function (Boltzmann distribution):

$$p(\theta) = \exp(-U(\theta)/kT) \quad (15)$$

where $U(\theta)$ is the potential energy of the dipole in the matrix. In a nematic matrix $U(\theta) = U'(\theta) - \mu E \cos\theta$, where $U'(\theta)$ is 0 in an isotropic medium and represents the local contribution of intermolecular interactions to the thermodynamic potential. In the Ising model, molecules are perfectly aligned, $\theta = 0$ or $\theta = \pi$, and $S = 1$, thus

$$\langle \cos^3\theta \rangle_{\text{Ising}} = \int_0^\pi p(\theta) \cos^3\theta \sin\theta \, d\theta / \int_0^\pi p(\theta) \sin\theta \, d\theta \quad (16)$$

$$= \int_0^\pi (\cos^3\theta) \exp(\mu E \cos\theta/kT) \times \exp(-U'(\theta)/kT) \sin\theta \, d\theta / \int_0^\pi \exp(\mu E \cos\theta/kT) \times \exp(-U'(\theta)/kT) \sin\theta \, d\theta \quad (17)$$

$$= \int_0^\pi (\cos^4\theta \mu E/kT + \ldots) \exp(-U'(\theta)/kT) \sin\theta \, d\theta / \int_0^\pi [1 + (\mu E \cos\theta/kT)^2/2 + \ldots] \times \exp(-U'(\theta)/kT) \sin\theta \, d\theta \quad (18)$$

The exponential functions are expanded and then reduced as follows. Keeping the first term in both expansion equations and neglecting the other terms for $\cos\theta = 1$ and $\mu E/kT \ll 1$

$$\langle \cos^3\theta \rangle_{\text{Ising}} = \int_0^\pi (\mu E/kT) \exp(-U'(\theta)/kT) \sin\theta \, d\theta / \int_0^\pi \exp(-U'(\theta)/kT) \sin\theta \, d\theta \quad (19)$$

Corrosion Reactions of $YBa_2Cu_3O_{7-x}$ and $Tl_2Ba_2Ca_2Cu_3O_{10+x}$ Superconductor Phases in Aqueous Environments

Ji-Ping Zhou and John T. McDevitt*

Department of Chemistry and Biochemistry, University of Texas at Austin, Austin, Texas 78712

Received November 20, 1991. Revised Manuscript Received March 24, 1992

The chemical reactions leading to the decomposition of superconducting $YBa_2Cu_3O_{7-x}$ ($0 > x > 0.05$) in water solution and water vapor at different temperatures were investigated and the corrosion products were characterized using X-ray diffraction and scanning electron microscopy. Although the $YBa_2Cu_3O_{7-x}$ phase is stable in some nonaqueous solvents, it reacts readily with water, acids, carbon dioxide, and carbon monoxide. Samples of $YBa_2Cu_3O_{7-x}$ soaked in water solution at 25, 50, and 75 °C all produce $BaCO_3$ and CuO corrosion products as determined by X-ray powder diffraction studies. Although there is some evidence for the formation of small amounts of Y_2BaCuO_5 and Y_2O_3, the majority of the Y-containing corrosion products are produced as amorphous phases. Our studies suggest that "Y_2BaCuO_5" is formed with a metastable or distorted structure. Moreover, when $YBa_2Cu_3O_{7-x}$ was exposed to water vapor equilibrated at a temperature of 75 °C, $BaCO_3$ forms and increases in amount with exposure time. On the other hand, CuO and "Y_2BaCuO_5" form only in the initial stages of corrosion. For comparison, superconducting $Tl_2Ba_2Ca_2Cu_3O_{10+x}$ was also investigated, and similar results were obtained. Details related to the corrosion of these two high-T_c phases are discussed herein.

Introduction

High-T_c phases $YBa_2Cu_3O_{7-x}$ and $Tl_2Ba_2Ca_2Cu_3O_{10+x}$ are p-type superconductors due to insertion of excess oxygen into the inactive layers.[1,2] Mixed valence $Cu^{2+/3+}$ states are present within the CuO_2 sheets in both structures,[3-6] giving rise to one of the necessary conditions to suppress

(1) Cava, R. J.; Batlogg, B.; van Dover, R. B.; Murphy, D. W.; Sunshine, S.; Siegrist, T.; Remeika, J. P.; Rietman, E. A.; Zahurak, S.; Espinosa, G. P. *Phys. Rev. Lett.* **1987**, *58*, 1676.

(2) Suzuki, T.; Nagoshi, M.; Fukuda, Y.; Syono, Y.; Kikuchi, M.; Kobayashi, N.; Tachiki, M. *Phys. Rev. B.* **1989**, *40*, 5184.

(3) Capponi, J. J.; Chailout, C.; Hewat, A. W.; Lijay, P.; Marezio, M.; Nguyen, N.; Raveau, B.; Sopubeyroux, J. L.; Tholence, J. L.; Tournier, R. *Europhys. Lett.* **1987**, *3*, 1301.

0897-4756/92/2804-0953$03.00/0